THE UNIVERSITY OF MICHIGAN
COLLEGE OF ENGINEERING
Cast Metals Laboratory

Final Report

MICROSTRUCTURE CONTROL IN MOLYBDENUM DUCTILE IRONS

and 4

D. R. Askeland
P. K. Trojan

ORA Project 31084

under contract with:

CLIMAX MOLYBDENUM COMPANY OF MICHIGAN
ANN ARBOR, MICHIGAN

administered through:

OFFICE OF RESEARCH ADMINISTRATION ANN ARBOR

February 1969

encm
UMR0124

TABLE OF CONTENTS

LIST OF ILLUSTRATIONS

LIST OF ILLUSTRATIONS (Continued)

LIST OF ILLUSTRATIONS (Concluded)

SUMMARY

The co-existence of spheroidal graphite, vermicular-flake graphite, and carbide in a nominal 3% C; 4% Si; 1% Al; 2% Mo ductile cast iron has been established as a function of several processing variables. A model has been proposed which relates the degree of undesirable microstructure to the carbide chemistry. In general rapid cooling rates, higher molybdenum contents, and low aluminum contents appear to decrease the vermicular graphite. The microstructure also appears to become more insensitive to processing variation as the amount of molybdenum is increased. The use of CeMg FeSi as a nodularizer in conjunction with a strontium bearing ferrosilicon post inoculant offers the most promise for minimization of decayed graphite shape. Finally, mechanical property tests, micro probe surveys, and other chemistry variations would be recommended for future research with this family of ductile cast irons.

INTRODUCTION

The development of molybdenum-containing ductile cast irons for intermediate temperature service (1200-1500°F) has required a close examination of the parameters which affect the graphite shape and the occurrence of carbides. It has been previously reported that the desirable elevated temperature properties can be attributed to the presence of a complex iron-molybdenum carbide with a somewhat variable metal atom ratio (1). On the other hand, these same carbides detract from the room temperature ductility of the material.

The purpose of this investigation is therefore to study the casting variables which will change the shape, quantity, and distribution of both the carbide and graphite for the following ductile iron chemistry range:

C	3.00-3.50
Si	3.75-4.25
Mn	0.15-0.40
Al	0-1.20
Mo	2.0-4.0
Mg	0-0.045

A ductile cast iron microstructure will be dependent upon a number of variables. In brief several of these are:

1. Melt history—includes input materials, melting technique, atmosphere, nodularizing, and post inoculant temperatures.

2. Chemistry—input materials and ladle additions.

3. Cooling rate—basically during solidification although some effect may also be noted in the solid state.

Unfortunately all of the variables are interrelated. However, if the melt history is held constant the general effects of chemistry and cooling rate can be studied. The investigation therefore emphasizes the metallographic variation in the carbide-graphite relationship as a function of:

Nodularizer type
Post inoculant type
Cooling rate
Chemistry variation
Heat treatment

EXPERIMENTAL PROCEDURE

Previous work at the Cast Metals Laboratory has resulted in a processing procedure for ductile cast iron which would allow critical evaluation of the variables as outlined above (2).

MELTING

The raw materials used in the investigation are given in Table I. The pig iron, high purity silicon, electrolytic manganese, ferro-molybdenum, and Armco iron are charged to a 3000-cycle, 115-lb capacity, alumina-lined induction furnace. Since all of the material cannot be charged at once, some pig iron is withheld until the initiation of melting, as which time the remainder is added to the partially molten bath.

When the metal is completely molten, 2 lb of CaC_2 (nut size) is added as a protective cover for the melt. The power is turned off when the melt reaches 2900°F and the CaC_2 is removed. The aluminum addition is then made by plunging pure ingot (except in those cases where aluminum was added in conjunction with the nodularizer). Upon cooling to 2750°F, the metal is treated with the magnesium alloy in an open ladle by the transfer technique. The post inoculant is added to the furnace (0.50% Si added) and the metal is poured back into the furnace which insures excellent mixing and solution of the post inoculant.

Finally the metal is tapped into a teapot ladle for pouring.

MOLDING AND POURING PROCEDURES

The molds poured and their descriptions are listed below:

Casting No.	Mold Material	Comments
1	6 mm bore Vycor	Chem sample before nodularization
2	6 mm bore Vycor	Chem sample after nodularization
3	6 mm bore Vycor	Chem sample after post inoculation
4	Dry sand	1/4" Y-block ┐
5	Dry sand	1/2" Y-block ├ in one flask
6	Dry sand	1" Y-block ┘ Fig. 1
7	Dry sand	1/4" Y-block ┐
8	Dry sand	1/2" Y-block ├ in one flask
9	Dry sand	1" Y-block ┘ Fig. 1
10	Core sand-graphite	Chem sample—1" dia coupons
11	Dry sand	3" Y-block
12	Core sand	Chill wedge ┐
13	Core sand	Chill wafer ├ Fig. 2
14	Steel	1" dia round ┘

The dimensions of the Y-block sections are shown in Fig. 1. The sand composition used for the Y-blocks was 4% western bentonite, 0.3% dextrin, 0.3% wood floor, and 3.5% water. The molds were dried for 12 hours at 300°F before being poured. The chill wafer was poured against a graphite plate while the chill wedge cooled most rapidly at the acute angle of the triangular cross-section (Fig. 2). The round chill was cast in a steel mold which provided a very rapid cooling rate. In several heats, liquid metal was poured directly into water to determine the effects of excessive cooling rates.

The entire set of castings (nos. 4-14) was poured in less than 60 sec. The pouring temperature for all heats was controlled within the range of 2550-2600°F. Temperature indication was with an immersion Pt-Pt 10% Rh thermocouple.

The diagram below schematically represents the variables considered.

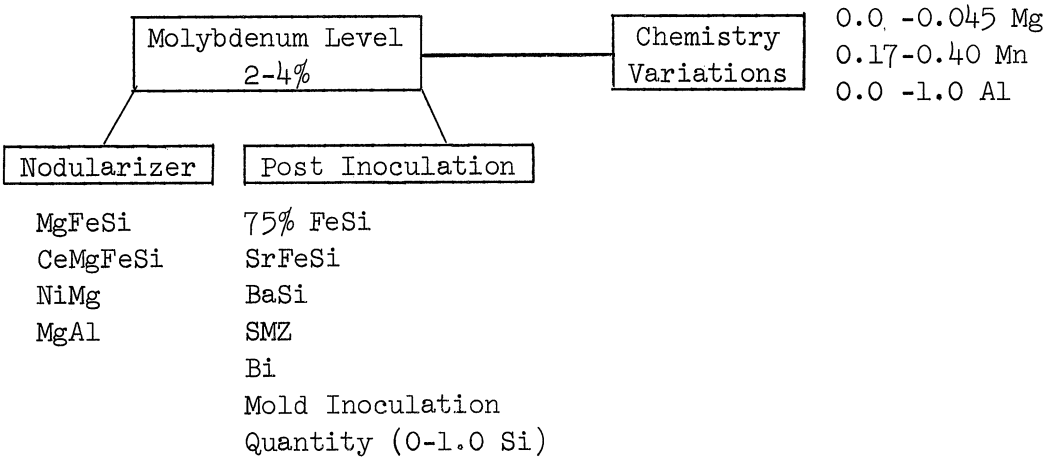

RESULTS AND DISCUSSION

The chemical analyses and scope of the heats poured are shown in Table II. The first series of heats was poured at the 4% Mo level while the last was at 2% Mo.

The microstructure would be expected to change as the cooling rate varied. It was therefore of interest to know the exact cooling rate for each of the Y-blocks. Thermocouples were placed at the thermal center of each section as shown in Fig. 1. The corresponding cooling curves are shown in Fig. 3. The solidification time was broad; from less than 1/2 min in the 1/4" Y-block to 15 min in the 3" Y-block. The experimental cooling curves were obtained for heat no. 9.

Since the major portion of the study was based upon a microstructural evaluation, the 1/2" Y-block from each heat was sectioned in order to compare the graphite-carbide quantity, shape, and distribution.

Figures 4 and 5 may be considered as somewhat representative of the 1/2" Y-block microstructures at the 2% and 4% Mo level. In general the amount of carbide and the vermicular graphite appear to increase as the amount of molybdenum is increased. The response of the two molybdenum levels to change in the processing variables is also different. Therefore the 4% Mo series will be considered first in the following sequence:

1. Section Sensitivity
2. Effects of Nodularizer and Post Inoculant
3. Effect of Metal Chemistry
4. Heat Treatment Response

4% Mo SERIES

1. Section Sensitivity

The extreme differences in cooling rates as shown in Fig. 3 should indicate variations in the microstructure. An example of the section size dependency is shown in Figs. 5 and 6. Both the 1/2" and 3" sections showed carbide and decayed graphite in conjunction with the desired spheroidal graphite shape. Of course the nodule count or graphite nucleation sites are seen to be lower in the 3" section. Also the amount of nonspheroidal or decayed graphite is greater in the larger section.

It is a well known phenomenon that processing variables which effect graphite size will also effect the carbide size. Therefore it should be noted that

the size of the carbide is also greater in the large 3" section. The occurrence of the upgraded graphite flakes or vermicular graphite in these sections is probably due to the graphitization of the larger carbides; a subject which will be discussed more fully in terms of the response to heat treatment.

2. Effects of Nodularizer and Post Inoculant

All combinations of nodularizer and post inoculant resulted in carbide and some decayed graphite shape in all section sizes. Most of the variation is subtle as can be seen by comparison of Figs. 5 and 7. The substitution of nickel-magnesium as the nodularizer has resulted in less carbide at the possible expense of larger quantities of decayed graphite. Since nickel is a graphitizer, the breakdown of the carbide might be anticipated. (The residual nickel in solution was 0.50.)

Research over the past few years has shown that additions of late silicon and mold inoculation can increase the nodule count and thereby decrease the carbide. More recently the addition of small quantities of bismuth in conjunction with a cerium bearing nodularizer have shown excellent nodularity and nodule counts in unalloyed ductile irons (3). Therefore 0.02 Bi was added with a strontium bearing ferrosilicon to a CeMgFeSi treated melt. The metal was then poured into Y-block sections which contained 0.02 Si as 85% FeSi (28-140 mesh). The resultant structure for a 1/2" Y-block is shown in Fig. 8. The indicated nodularity was the best obtained at the 4% Mo level. However the skeletal carbides still persist. It should again be noted that high nodule counts resulted in a finer carbide structure.

As was pointed out in a previous progress report, even though carbide could not be suppressed at the 4% molybdenum level, graphite would still occur in chilled sections (4). This phenomenon is probably associated with the high silicon content, although it is also dependent upon when the silicon is added; as will be discussed in a later section.

3. Effects of Metal Chemistry

The stabilization of carbide by magnesium has been well documented in the literature. This appears to hold true for the primary solidification product, however the effect has not been well established for the occurrence of carbide over graphite as the eutectic product. In order to determine the carbide stabilization by magnesium, two special heats were conducted. Figure 9 shows the microstructure of a 1/2" section with no magnesium added while Fig. 10 illustrates the result of undertreatment with magnesium (0.01 Mg residual). In both cases the amount of carbide has not changed significantly. Of course the degree of graphite nodularity is seen to be less than in the previous figures. The higher magnification used in Fig. 9 is particularly interesting in that

the primary graphite appears to have stable eutectic carbide in very close association with no tendency for carbide dissociation.

Two other elements were studied to evaluate their relationship to the microstructure. Figure 11 shows a 1/2" Y-block in which the manganese was reduced by one-half. The normal manganese (0.35) is shown in Fig. 5. The amounts of carbide appear to be identical. It is interesting to note however that lower manganese gives an increase in the amount of fine decayed graphite closely associated with the eutectic carbide.

Finally a heat was poured with no aluminum and is shown in Fig. 12. Since previous data had shown some benefit of mold inoculation, the particular 1/2" Y-block shown had been inoculated in the mold with 85% FeSi; besides the normal 0.50 Si added as a post inoculant. Again, both carbide and vermicular graphite are seen to be present. It is however possible that the amount of carbide may be less when no aluminum is present.

4. Heat Treatment Response

It is apparent from the preceding discussion that the eutectic or skeletal carbides are difficult to destroy at the 4% Mo level. Since the normal variation in liquid metal processing had very little effect, a series of heat treatments was conducted to evaluate the carbide thermal stability and to determine if, first stage graphitization could be obtained. Two temperatures, 1750°F and 1850°F for two hours and an air cool, were selected for the microstructural comparison. As an extreme, NiMg + SrFeSi and CeMgFeSi + 75 FeSi treatments were compared in 1/4" and 3" sections. As cast microstructures of these chemistries had been previously shown for 1/2" Y-block sections in Figs. 3, 5, and 7.

Figures 13-15 illustrate the response to heat treatment of 1/4" sections for the nickel bearing nodularizer while Figs. 16 and 17 are the corresponding sections for the cerium bearing nodularizer. In general the nodularity is quite good for both materials. There appears to be no graphitization during the heat treatment. Therefore, any breakdown of carbide is associated with the growth of existing graphite to produce "wings" as seen in Figs. 14, 15, and 17. On the other hand the skeletal carbides are not destroyed at 1850°F for 2 hours.

The 3" Y-block sections after heat treatment are shown in Figs. 18-22. The original as cast structures in the 3" sections contained vermicular and flake graphite which persisted in the heat treated samples. Again there is little evidence of solid state graphitization and the skeletal carbides still remain. Figure 20 however does indicate some possible spheroidization of what had previously been a skeletal carbide. The presence of nickel may have enhanced the spheroidization in this particular specimen.

Several of the phenomenae reported earlier do not appear to be present in the above series. In particular there is little or no evidence of a loss in the decayed graphite shape or in the quantity of graphite (4). The heat treatment however may break up the continuity of carbide, therefore the normalizing treatment may be beneficial.

Before an attempt at rationalization can be made for the heat treatment response, it is necessary to consider the parameters which characterize the lower or 2% Mo grade ductile cast iron. These latter materials have a more discontinuous skeletal carbide as indicated previously. Further, they appear to be much more sensitive to the experimental parameters than do the 4% Mo materials. The discussion below has therefore been subdivided into the same categories as presented for 4% Mo study.

2% Mo SERIES

1. Section Sensitivity

The general trend of more vermicular graphite and larger skeletal carbides in heavier sections as noted for the 4% Mo materials was again observed at the lower molybdenum contents. On the other hand, the "degree of graphite shape change" was found to be different for the two molybdenum levels. The nonspheroidal graphite present in the 3" Y-blocks had shorter lengths and more rounded tips in the 2% Mo castings than was found in the 4% Mo sections. This may be partially attributed to the relationship with the carbide which was also found to be less continuous at the lower molybdenum levels. A practical manifestation of the discontinuous carbide and stubbier vermicular graphite should be higher room temperature strengths and ductility.

It was possible to produce a structure with no graphite by quenching liquid metal droplets into a water bath. This however could only be accomplished if MgAl was used as the nodularizer and if all of the silicon was present in the original melt (Fig. 23). If large quantities of late silicon are added, the quenched metal droplets again contain graphite as seen in Fig. 24.

2. Effects of Nodularizer and Post Inoculant

Figures 25 and 26 can be compared with Fig. 4 to obtain a relative comparison of the ladle treatments. It would appear that CeMgFeSi in conjunction with SrFeSi provided slightly better nodularity. In general the continuity of the carbide has been difficult to evaluate when any of the nodularizers are used in combination with 0.50 late silicon added as any of the post inoculants. On the other hand if the amount of late silicon is changed, both the carbides and the graphite shape are affected. As an example, Fig. 27 is a microstructure where no late silicon was added. The graphite shape is much poorer than

would be anticipated if 0.50 silicon was added; as represented by Fig. 26 (the two nodularizers NiMg and MgAl react very similarly in their ability to retain graphite sphericity.) Even a small amount of late silicon as a mold inoculant (0.02 Si as 85% FeSi) can help to increase the nodularity as shown in Fig. 28.

The question then arises whether larger quantities of late silicon sould help the nodularity still further. Figure 29 where 1.0 late silicon was added appeared to show no benefit over a 0.50 Si addition. It may in reality be somewhat detrimental since some of the carbide may have graphitized.

It should also be pointed out that some graphite decay within the Y-block section generally meant a severe degeneration at the surface of the casting. Figure 30 represents the form of surface graphite degeneration which is found in MgAl and NiMg treated castings but seldom if ever found if the nodularizer is CeMgFeSi or MgFeSi.

3. Effects of Metal Chemistry

Only the effect of aluminum was evaluated at the low molybdenum level. Figure 31 shows zero aluminum to provide excellent nodularity although a poor nodule count (compare with Fig. 25 which had 1.0 Al). Here again however, the nodule count could be increased at little sacrifice in nodularity through the use of mold inoculation as shown in Fig. 32. It may also be possible that the lack of aluminum may decrease the amount of carbide which had been previously suggested for the 4% Mo alloy.

4. Heat Treatment Response

At this lower molybdenum level, the response to thermal decomposition of carbide was again studied at 1750 and 1850°F for 2 hours. The selected alloys had 0% and 1% Al with a MgFeSi nodularizer and 75% FeSi as the post inoculant. As mentioned previously, with no aluminum present the nodularity was excellent (Fig. 31). A 1/4" section after 2 hours at 1850°F is shown in Fig. 33. The nodularity is still good although the carbides persist. Figures 34 and 35 show the zero aluminum alloy in a 3" section have excellent nodularity after a 1750°F treatment. After 2 hours at 1850°F the carbides have spheroidized and vermicular graphite has appeared.

The alloy containing 1% Al has followed a similar pattern as shown in Figs. 36-38. It is difficult to determine if new vermicular graphite has occurred during the heat treatment since a great deal is present in the original as cast condition. It is felt however that the vermicular graphite has more rounded tips at 1850°F as compared to 1750°F. Finally as a check on the above point, a round cast in the steel mold (Fig. 2) was heat treated. Figure 39 shows the cast structure with a high nodule count and excellent nodularity.

Figure 40 taken after 6 hours at 1850°F again shows excellent nodularity with only a slight destruction of the eutectic form skeletal carbides. The graphite which formed was very stubby and short in length.

CARBIDE-GRAPHITE MECHANISM

The preceding discussion has been based upon a phenomenological analysis of several inter-dependent processing variables. The discussion would not be complete without some attempt at rationalization of the physical occurrences. Of course the problem is made extremely difficult by the relative insensitivity of this class of cast irons to changes in the casting process. In other words, chances are excellent that skeletal or eutectic carbide and vermicular or decayed graphite will occur under any given set of casting conditions. The problem then reduces to an evaluation of "degree of undesirable microstructure." It might also be mentioned that mechanical testing of several of the sections would facilitate the analysis. However in the absence of such data, several general effects may still be considered.

Recently a new proposed phase relationship has been presented for the Fe-C-Si system (5). Although the analysis has been somewhat complex, several interesting observations are noteworthy:

1. Castings constitute a nonequilibrium condition where carbides occur only within austenite formed either as a proeutectic or eutectic product.

2. Austenite rather than graphite or carbide is the phase which initiates eutectic transformation.

3. In hypoeutectic iron the eutectic freezing range is narrow, where proeutectic austenite promotes the occurrence of carbide. The incidence of graphite is from carbide dissociation.

4. In eutectic and hypereutectic iron the eutectic freezing range is broad where slow cooling not only promotes carbide dissociation to graphite but proeutectic graphite will also occur.

5. The relative ease of carbide dissociation is chemistry dependent and all carbide is not Fe_3C but rather can also be $Fe_{10}Si_2C_3$.

Of course the above results relate to the Fe-C-Si system and require a degree of bending to apply to the system which also contains molybdenum and aluminum. Therefore several assumptions must be made.

Since there is no exact way to measure the eutectic in the complex system or the temperature range over which four phases may coexist (austenite, graphite, carbide, and liquid), the chemistry will be assumed to be hypereutectic.

This is justified on the basis of the difficulty encountered in the attempt to suppress graphite formation. Finally the skeletal carbides occur at the eutectic from some of the last liquid to solidify. (The metallographic pattern would appear to support the assumption.)

In brief, graphite is nucleated first; the nodule count dependent upon nucleation sites furnished through under cooling or post inoculants. Austenite then nucleates the eutectic reaction as in the Fe-C-Si system. However the presence of molybdenum is known to increase the carbide stability and decrease the carbon saturation level of the austenite as shown by several isopleths at constant molybdenum contents (Fe-C-Mo system). Therefore, the surrounding liquid becomes enriched in molybdenum and carbon until a carbide must form rather than nucleation of graphite or growth of the existing graphite nuclei. It is then this carbide which may dissociate to graphite that results in much of the vermicular or flake graphite shapes.

If the carbide is high enough in molybdenum it is stable and does not graphitize. If on the other hand the carbide also contains silicon and low molybdenum, it is prone to graphitization but only to the extent where the remaining carbide becomes enriched in molybdenum to the point where it stabilizes. In other words the austenite is already saturated with molybdenum, therefore the destruction of some carbide requires an enrichment of the remaining carbide. This then explains the observed close association between carbide and graphite with no tendency for carbide dissociation.

It should then be evident from the above model that carbide and graphite will always be present in these alloys; which was experimentally determined to be the case. However it would also be useful to now review several of the observed phenomenae and relate them to the proposed model.

1. Light sections have less decayed graphite, and more continuous carbide which resists thermal decomposition. Due to the short diffusion paths, any carbide dissociation may therefore find growth of existing graphite nuclei easier than nucleation of new graphite. The eutectic carbides may also be higher in molybdenum and lower in silicon when the cooling rate is rapid; which would then inhibit dissociation.

2. In an opposite sense, the heavier sections have more decayed graphite where carbide spheroidization and thermal decomposition is more readily accomplished. Again diffusion versus nucleation would appear to rationalize the occurrence.

3. Higher molybdenum contents appear to present at least as good if not better nodularity. Furthermore, the more continuous carbides become very resistant to graphitization. If the carbide contains more molybdenum it should in fact inhibit dissociation; both during cooling and during heat treatment.

4. The presence of aluminum increases the quantity of carbide and also increases the amount of vermicular graphite. There are a number of ways in which the observation may be rationalized. Unfortunately the effect of aluminum on silicon, carbon, and molybdenum solubility in both austenite and carbide must be assumed in order to provide a logical answer. That aluminum does have an effect on these phase compositions is the only way to justify the experimental results. It should also be recalled that low aluminum gave much better nodularity at the 2% Mo level and offered a much lesser effect at 4% Mo.

5. Variations in manganese and magnesium do not appear to extensivety change the carbide stability. This may have been anticipated in that the chemistry variations have been minor. Manganese in fact has been noted for a much more pronounced effect on secondary graphitization of pearlitic carbide rather than on eutectic carbide. On the other hand, 4% Mo plus low Mn did appear to exhibit excessive graphite degeneration when compared to higher manganese contents.

6. Some combinations of nodularizer and post inoculant have been found to provide a more desirable microstructure. If the previous arguments of short diffusion paths as being desirable are valid, such things as "strong post inoculants" and mold inoculation should provide more nucleation sites for graphite and creat a more stable carbide. It is also curious that bismuth was not as effective at the lower molybdenum level. Finally no late silicon was detrimental as were large quantities of late silicon; all of which suggest an interdependency between nucleation of graphite and ultimate growth of a carbide which can have varying chemistry.

To say the least, the proposed model and observed results are not very satisfying in the light of the desired objectives of the research. However it is felt that some insight into the complexity of the problem has been achieved Finally, the course of future research on the alloy system has also been described by the present experimental results.

CONCLUSIONS AND RECOMMENDATIONS

A broad variation in nodularizers, post inoculants, cooling rates, and several chemical elements has resulted in a graphite-carbide model and the following observed phenomena.

1. Rapid cooling rates promote more continuous carbide and better graphite nodularity.

2. Higher molybdenum contents may also increase the nodularity through stabilization of carbide which can decay to vermicular shapes.

3. Low aluminum contents provide less carbide and increase the nodularity; particularly at lower molybdenum levels.

4. Combinations of nodularizers and post inoculants which increase the nodule count inhibit vermicular graphite. CeMgFeSi in conjunction with strontium bearing ferro silicon gives the best nodularity in the presence of aluminum.

5. Mold inoculation appears to decrease the amount of vermicular graphite.

6. Zero late silicon or 1% late silicon appear to increase the amount of vermicular graphite.

7. Carbide produced in heavy sections will partially dissociate to poor graphite shapes during a normalizing treatment whereas carbide from light sections resists thermal decomposition.

The following recommendations may then be made:

1. Mechanical tests of several of the representative carbide-graphite combinations should allow quantification of the microstructural variations.

2. The proposed model for the carbide-graphite interaction could be expanded through a microprobe analysis.

3. A series of heats with variable silicon contests would aid the understanding of the phase relationships.

4. Selected elements could be added to the base material in order to change the shape, distribution, and molybdenum content of the carbide. These might include such elements as Cr, Co, or possibly higher Mn.

BIBLIOGRAPHY

1. Sponseller, D. L., Scholz, W. G., and Rundle, D. F., "Development of Low-Alloy Ductile Iron for Service at 1200-1500°F," Trans. Amer. Fndrymn's Soc., 76, 353-368 (1968).

2. Trojan, P. K., Bargeron, W. N., and Flinn, R. A., "The Evaluation of Nodularizers and Post Inoculants for Ductile Iron," Trans. Amer. Fndrymn's Soc., 75, 611-624 (1967).

3. Sawyer, J. C., and Wallace, J. F., "Effects and Neutralization of Trace Elements in Gray and Ductile Irons," Trans. Amer. Fndrymn's Soc., 76, 386-404 (1968).

4. Askeland, D. R., and Trojan, P. K., "Microstructure Control in Molybdenum Ductile Irons," ORA Report 31084-1-P, November 1968.

5. Olen, K. R., and Heine, R. W., "A Revision of the Fe-C-Si System," Trans. Amer. Fndrymn's Soc., 76, 369-384 (1968).

TABLE I

CHEMICAL ANALYSES OF RAW MATERIALS

Material	% C	% Si	% Mn	% P	% S	% Mg	% Mo	% Al	% Sr	% Ni	% Ce	Others
Pig Iron A	4.25	—	.08	.022	.015	—	—	—	—	—	—	.020 Ti
Pig Iron B	4.55	.60	.20	.017	.016	—	—	—	—	—	—	—
Armco	.015	.003	.03	.005	.025	—	—	—	—	—	—	—
CeMgFeSi	—	48.2	—	—	—	8.60	—	.93	—	—	.51	1.20 Ca
NiMg	—	31.2	—	—	—	14.65	—	—	—	50.1	—	.06 Cu
MgFeSi	—	46.5	—	—	—	8.49	—	.75	—	—	—	1.48 Ca
Al Mg	—	—	—	—	—	14.47	—	Rem.	—	—	—	—
75% FeSi	—	75.94	—	—	—	—	—	1.30	—	—	—	1.05 Ca
SrFeSi	—	69.63	—	—	—	—	—	.85	.88	—	—	.09 Ca
FeMo	.03	.45	—	.05	—	—	62.0	—	—	—	—	—
Al Metal	—	—	—	—	—	—	—	99.9	—	—	—	—
Si Metal	—	98.98	—	—	—	—	—	.09	—	.01	—	.54 Fe
Elec. Mn	—	—	99.95	—	.023	—	—	—	—	—	—	.20 O
BaSi	—	50.0	—	—	—	—	—	—	—	—	—	Rem. Ba

TABLE II

HEAT CHEMISTRIES AND PURPOSE

Heat No.	Nodulizer	Post Inoculant	% C	% Si	% Mn	% Mo	% Al	% Mg	Comments
				4% Mo Series					
2	MgFeSi	75% FeSi	3.16	4.28	.29	4.10	1.22	.041	
3	CeMgFeSi	74% FeSi	3.22	3.50	.46	4.20	1.37	.042	
4	CeMgFeSi	SrFeSi	3.20	4.26	.39	3.96	1.06	.031	
5	NiMg	SrFeSi	3.32	4.23	.37	4.10	1.03	.033	
6	MgAl	SrFeSi	3.49	4.03	.33	4.12	.91	.031	
7	CeMgFeSi	BaSi*	3.27	4.11	.37	4.20	1.00	.033	
8	None	75% FeSi*	3.52	4.49	.35	3.88	.74	None	No Mg added
9	MgFeSi	75% FeSi*	3.48	4.34	.30	3.75	.84	.011	Low Mg heat
10	CeMgFeSi	75% FeSi*	3.66	4.17	.17	3.75	.90	.024	Low Mn heat
11	CeMgFeSi	SrFeSi*	3.56	4.39	.39	3.62	.87	.021	.02 Bi added
12	MgFeSi	75% FeSi*	3.54	3.84	.42	3.95	--	.024	No Al added
				2% Mo Series					
13	MgFeSi	75% FeSi*	3.52	4.17	.46	2.28	1.11	.033	
14	MgFeSi	75% FeSi*	3.48	4.05	.42	2.40	--	.038	No Al added
15	CeMgFeSi	SrFeSi*	3.35	3.82	.39	2.25	1.14	.033	
16	NiMg	SrFeSi*	3.38	3.79	.34	2.20	1.13	.037	
17	MgAl	SrFeSi*	3.32	3.99	.46	2.22	1.11	.036	
18	CeMgFeSi	SrFeSi*	3.35	4.04	.35	2.05	1.18	.032	.02 Bi added
19	MgAl	None*	3.39	3.63	.40	2.12	.75	.031	
20	CeMgFeSi	SMZ*	3.34	3.87	.42	2.12	1.13	.031	1.0 Si added late

Note: Sulfur and phosphorus less than 0.020 for all heats.
*0.02 Si added as 85% FeSi (-28 +140 mesh) to molds 7, 8, and 9.

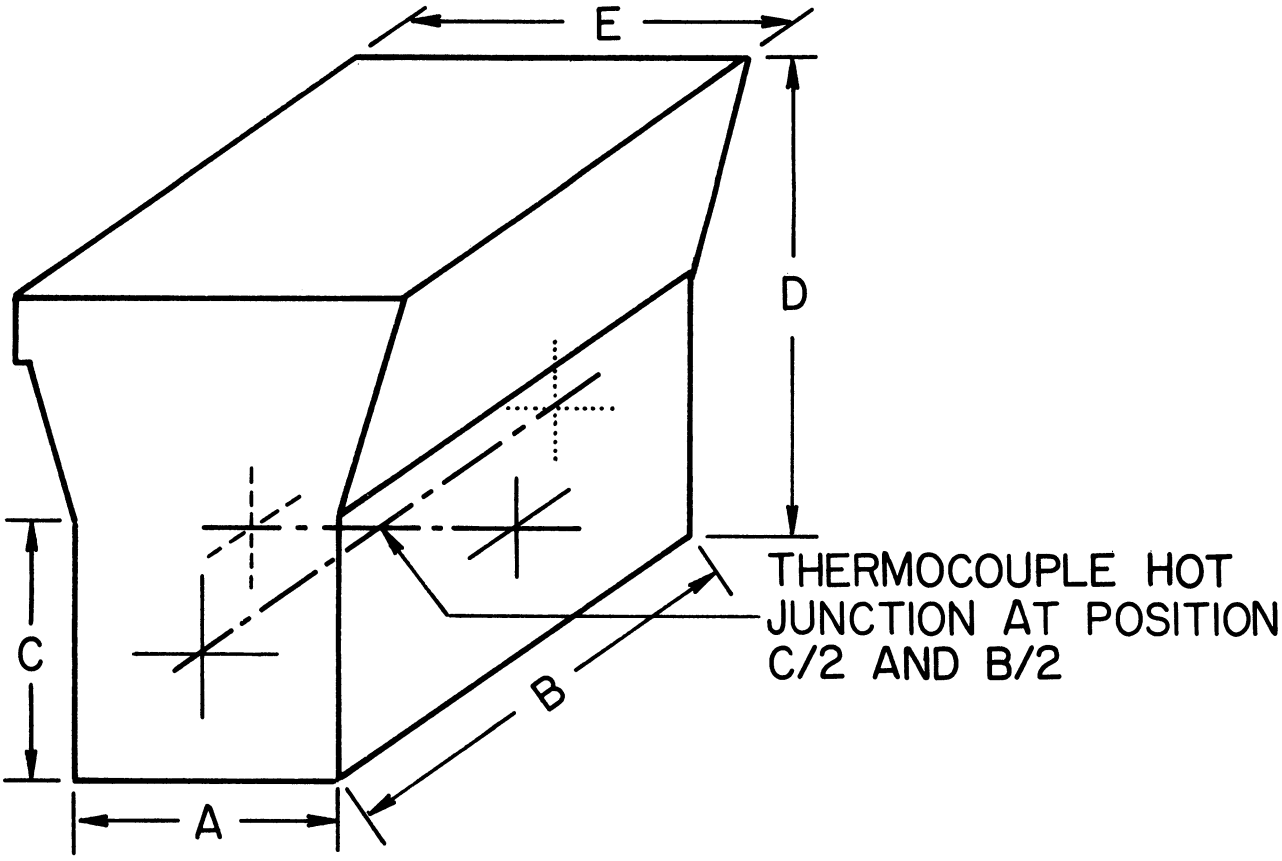

Y-BLOCK (INCHES)	A (IN.)	B (IN.)	D (IN.)	C (IN.)	E (IN.)
3	3	6	5 1/2	2 1/2	4 3/4
1	1	6	4 1/4	1	2
1/2	1/2	6	3 1/2	1	1 1/2
1/4	1/4	6	2	1/2	1 3/4

Fig. 1. Y-block design, dimensions, and thermocouple placement.

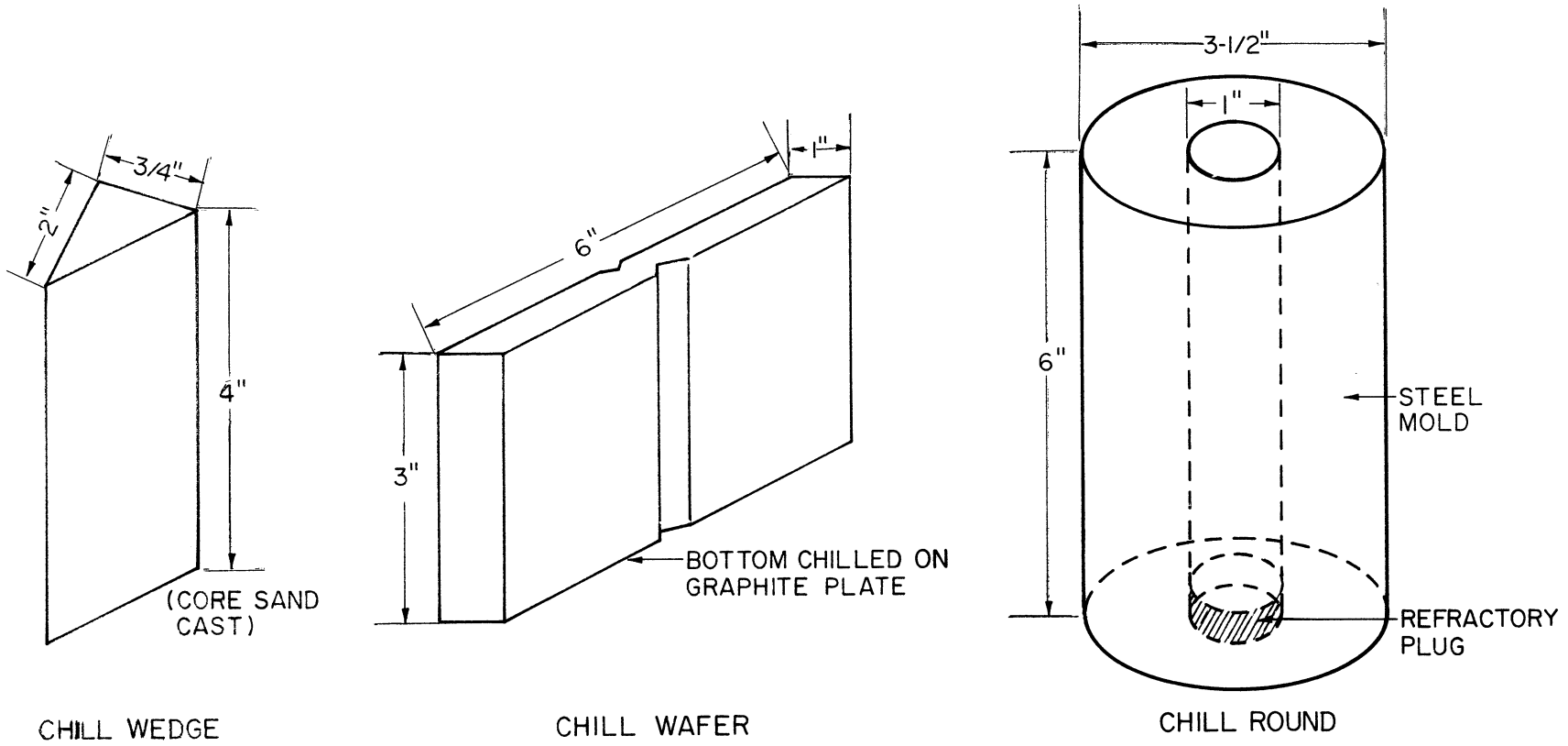

Fig. 2. Chill wedge, wafer, and round dimensions and design.

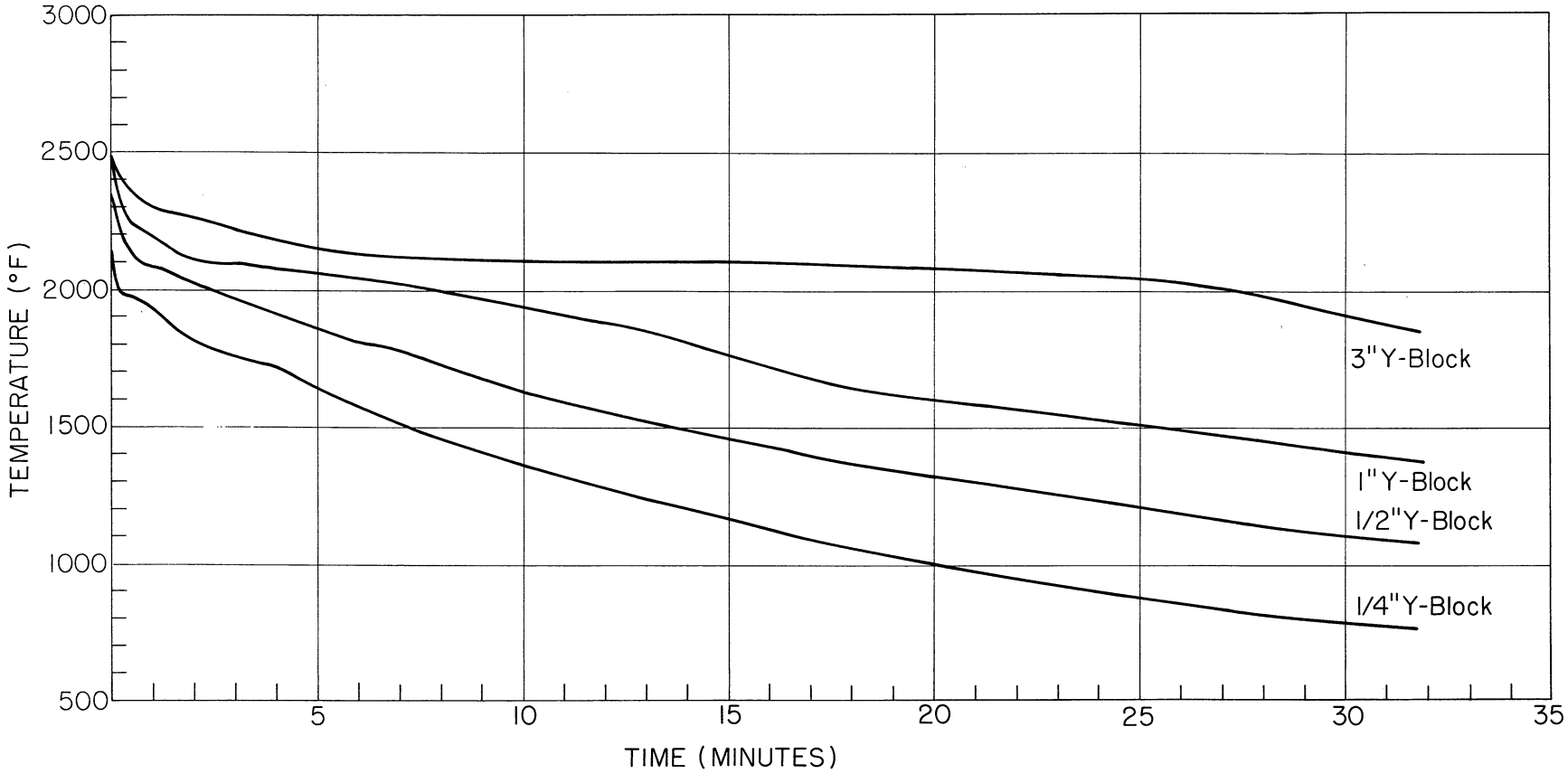

Fig. 3. Cooling curves for Y-block sections.

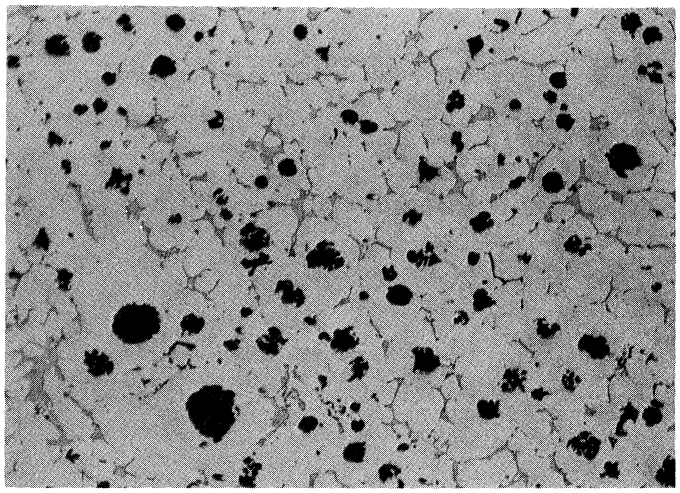

Fig. 4. 100X. 1/2" Y-block. CeMgFeSi; SrFeSi; 2% Mo; 1% Al level. Heat 15.

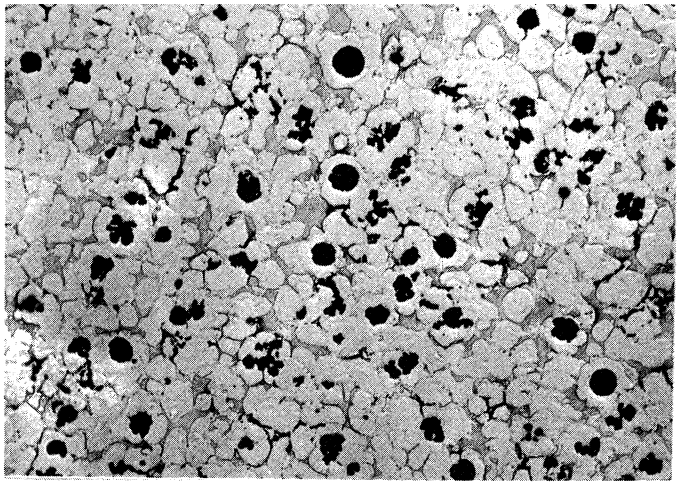

Fig. 5. 100X. 1/2" Y-block. CeMgFeSi; 75% FeSi; 4% Mo; 1% Al level. Heat 3.

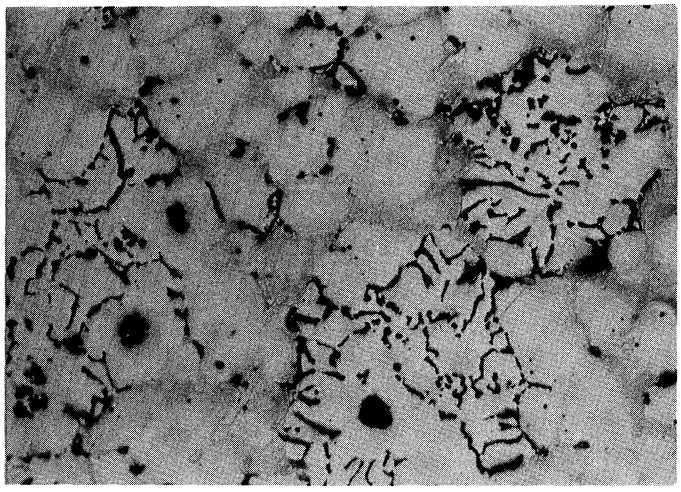

Fig. 6. 100X. 3" Y-block. CeMgFeSi; 75% FeSi; 4% Mo; 1% Al level. Heat 3.

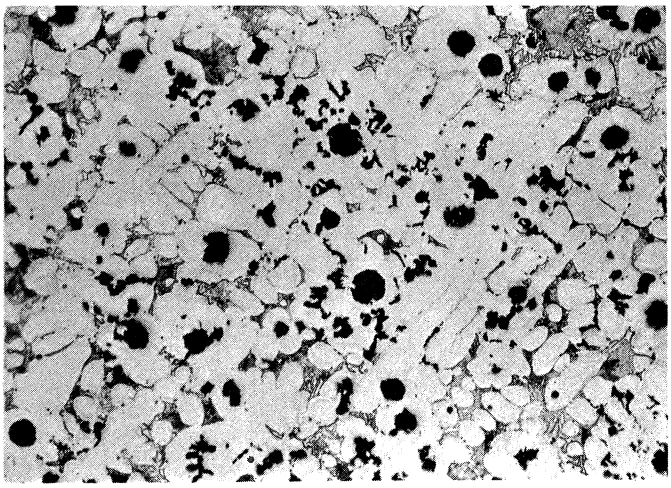

Fig. 7. 100X. 1/2" Y-block. NiMg; SrFeSi; 4% Mo; 1% Al level. Heat 5.

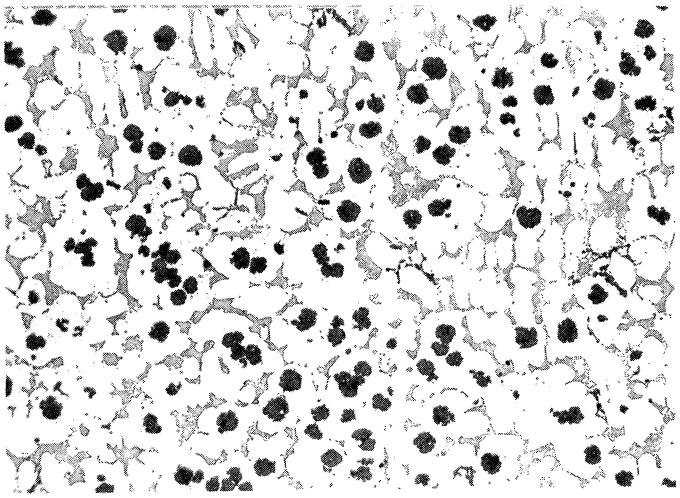

Fig. 8. 100X. 1/2" Y-block. CeMgFeSi; SrFeSi; 0.02 Bi plus mold inoculation; 4% Mo; 1% Al level. Heat 11.

Fig. 9. 500X. 1/2" Y-block. No magnesium added; 75% FeSi. Heat 8.

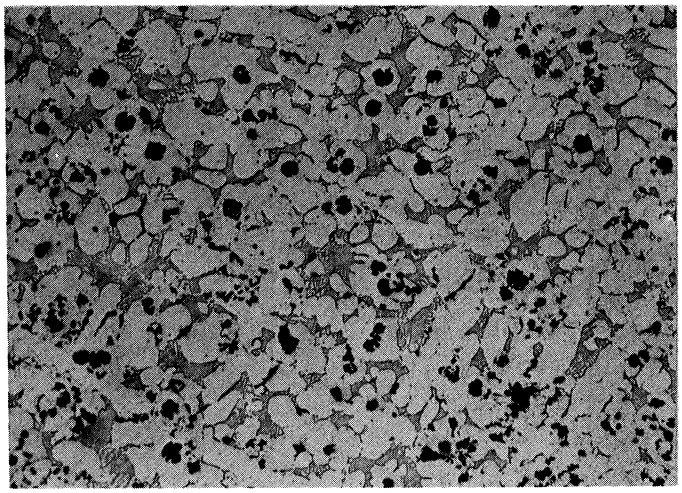

Fig. 10. 100X. 1/2" Y-block. MgFeSi; 75% FeSi; 0.011 residual magnesium; 4% Mo; 1% Al level. Heat 9.

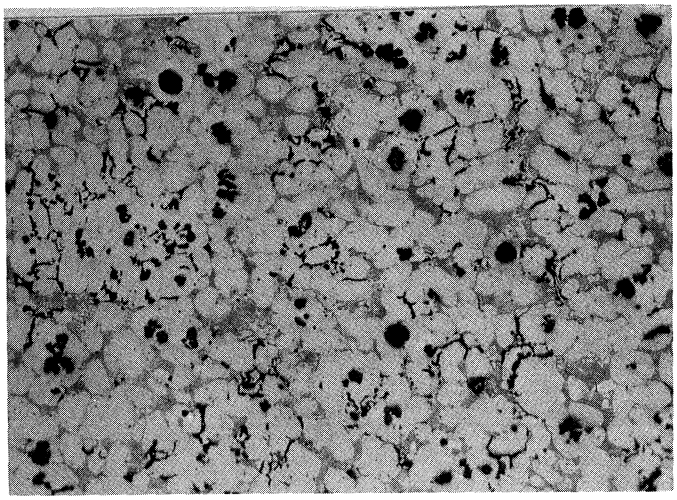

Fig. 11. 100X. 1/2" Y-block. CeMgFeSi; 75% FeSi; low manganese (0.17); 4% Mo; 1% Al level. Heat 10.

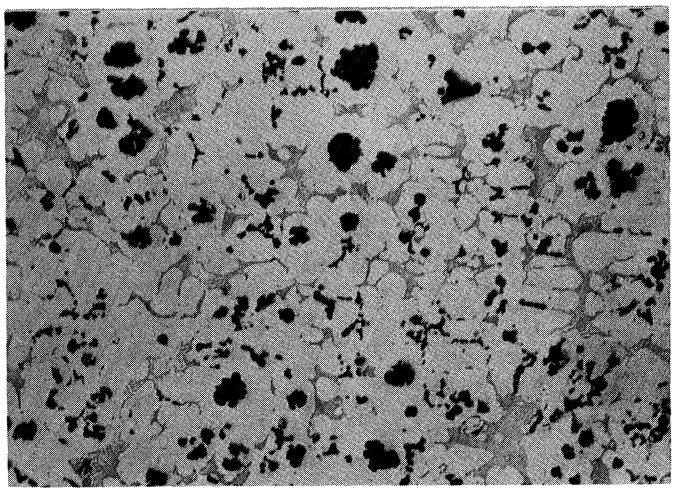

Fig. 12. 100X. 1/2" Y-block MgFeSi; 75% FeSi; mold inoculation; 4% Mo; 0% Al level. Heat 12.

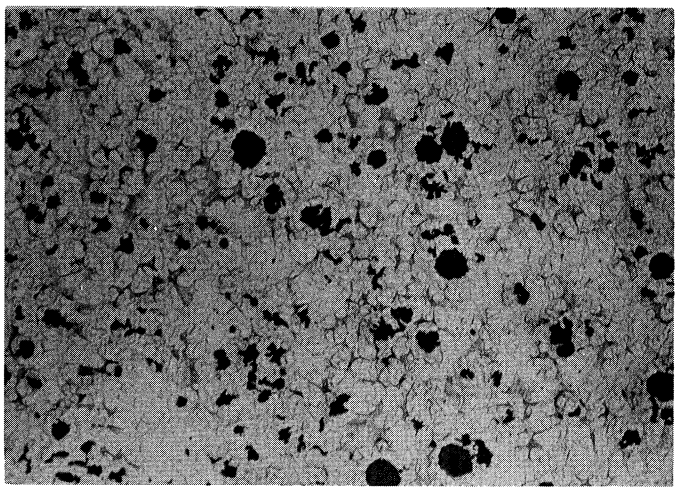

Fig. 13. 100X. 1/4" Y-block. Normalized 2 hours at 1750°F; NiMg; SrFeSi; 4% Mo; 1% Al level. Heat 5.

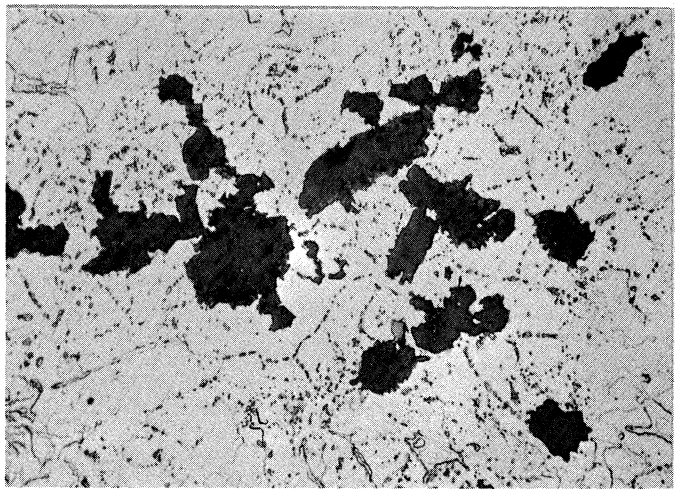

Fig. 14. 500X. 1/4" Y-block. Higher magnification of Fig. 13.

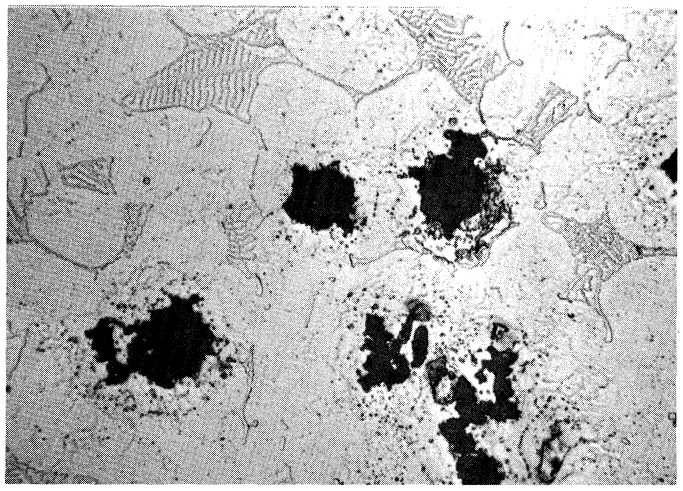

Fig. 15. 500X. 1/4" Y-block. Normalized 2 hours at 1850°F; NiMg; SrFeSi; 4% Mo; 1% Al level. Heat 5.

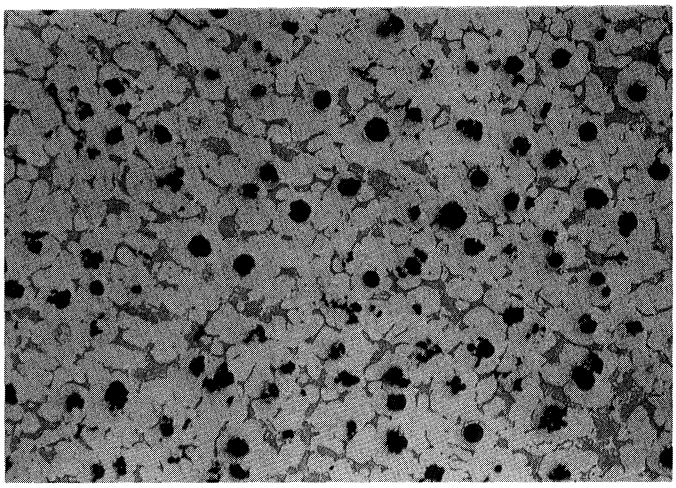

Fig. 16. 100X. 1/4" Y-block. Normalized 2 hours at 1850°F; CeMgFeSi; 75% FeSi; 4% Mo; 1% Al level. Heat 3

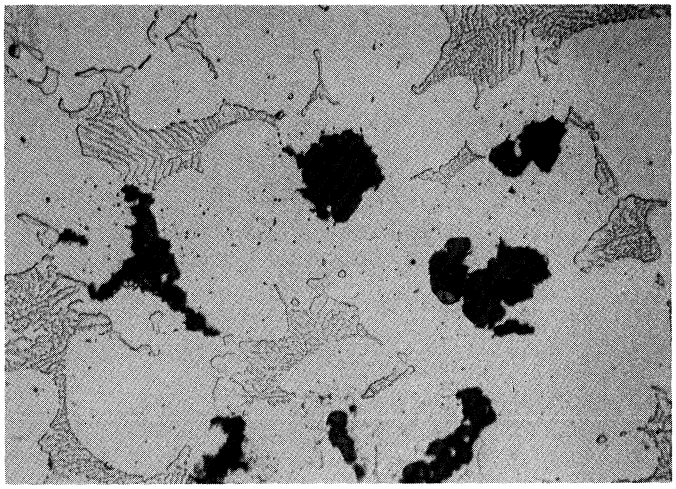

Fig. 17. 500X. 1/4" Y-block. Higher magnification of Fig. 16.

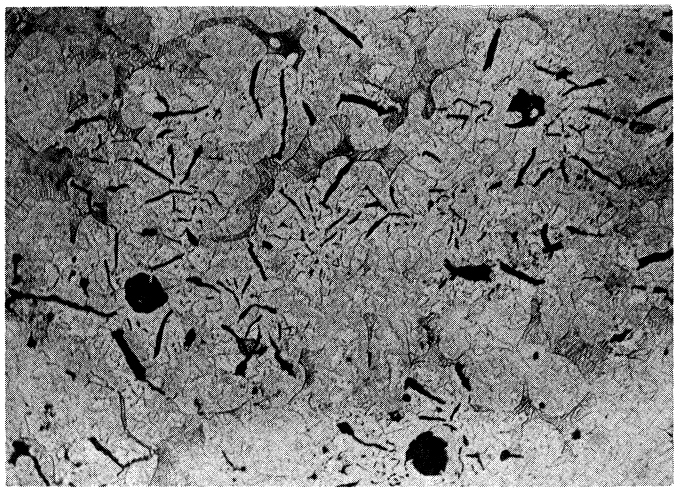

Fig. 18. 100X. 3" Y-block. Normalized 2 hours at 1750°F; NiMg; SrFeSi; 4% Mo; 1% Al level. Heat 5.

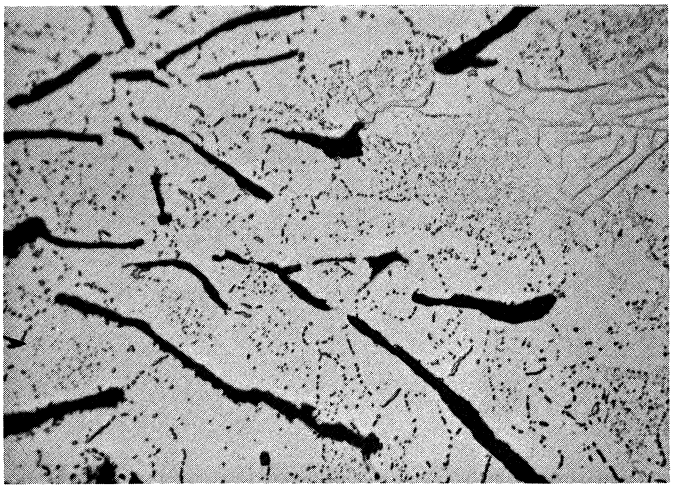

Fig. 19. 500X. 3" Y-block. Higher magnification of Fig. 18.

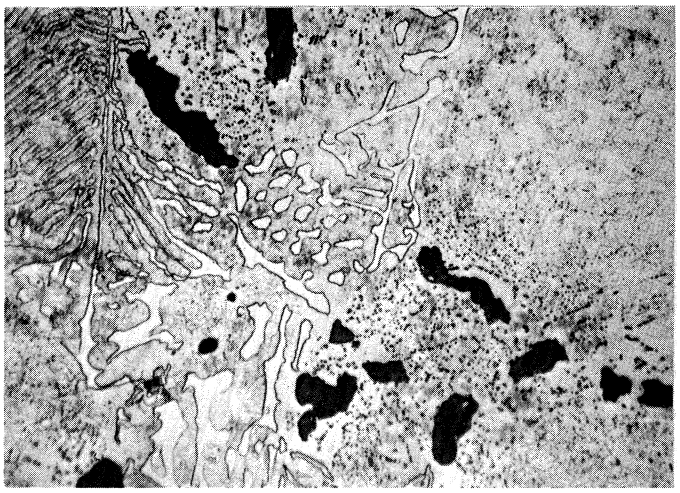

Fig. 20. 500X. 3" Y-block. Normalized 2 hours at 1850°F; NiMg; SrFeSi; 4% Mo; 1% Al level. Heat 5.

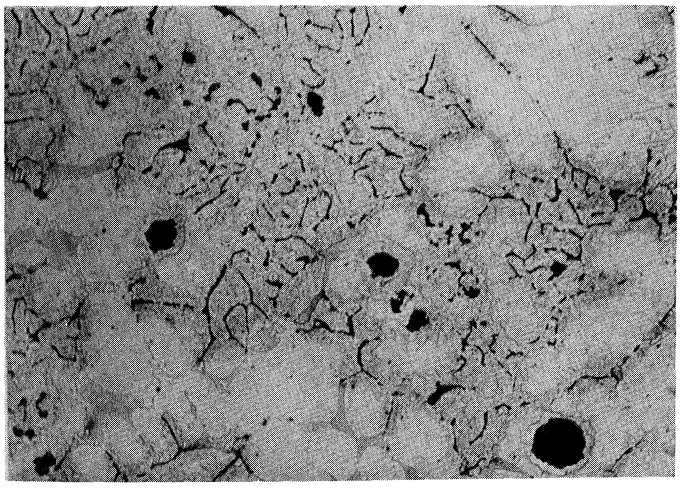

Fig. 21. 100X. 3" Y-block. Normalized 2 hours at 1850°F; CeMgFeSi; 75% FeSi; 4% Mo; 1% Al level. Heat 3.

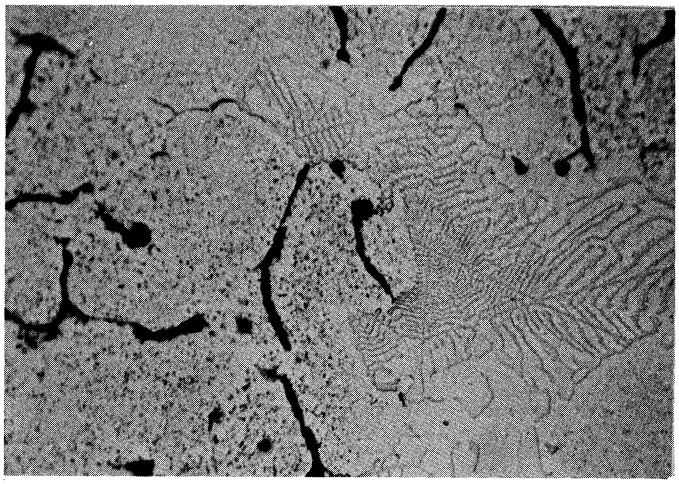

Fig. 22. 500X. 3" Y-block. Higher magnification of Fig. 21.

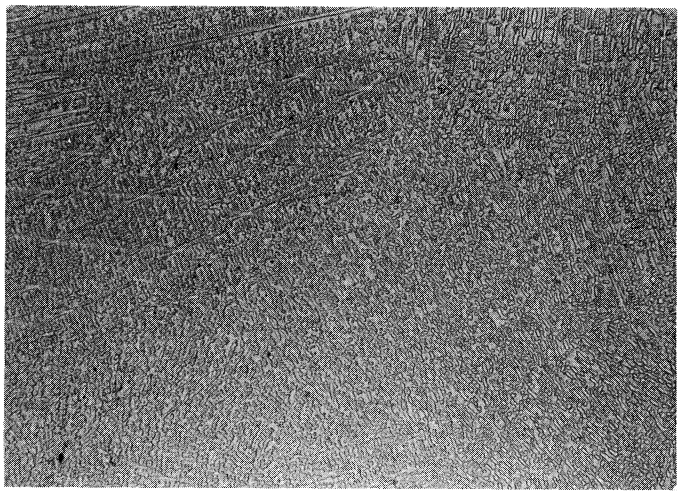

Fig. 23. 100X. Water quenched pellets. MgAl; no late silicon added; 2% Mo, 1% Al level. Heat 19.

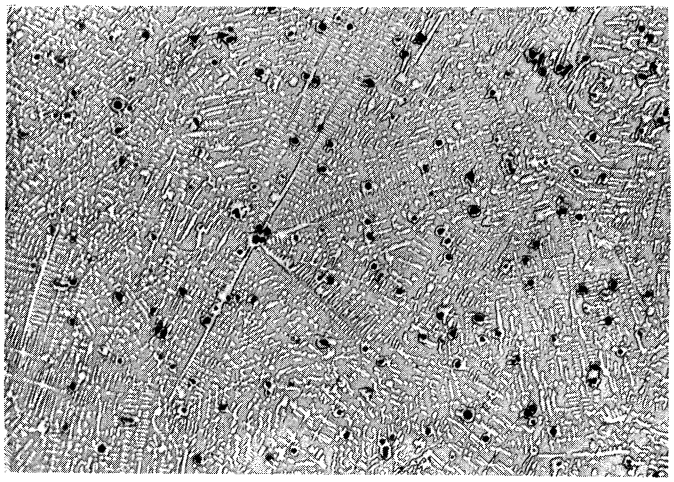

Fig. 24. 100X. Water quenched pellets. CeMgFeSi; SMZ (1% Si added late); 2% Mo; 1% Al level.

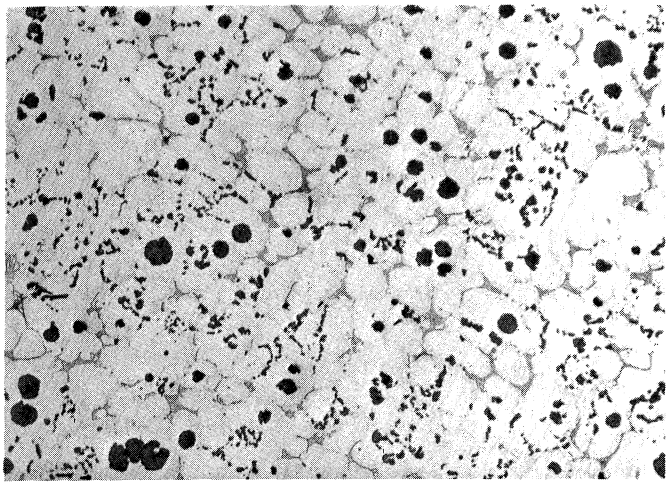

Fig. 25. 100X. 1/2" Y-block. MgFeSi; 75% FeSi; 2% Mo; 1% Al level. Heat 13.

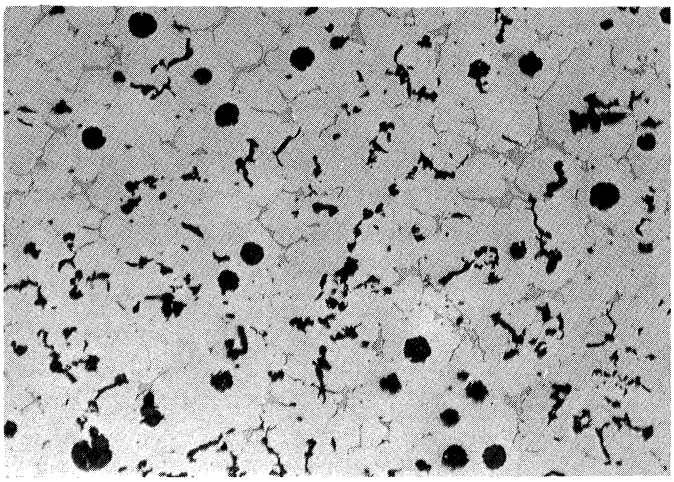

Fig. 26. 100X. 1/2" Y-block. NiMg; SrFeSi; 2% Mo; 1% Al level. Heat 16.

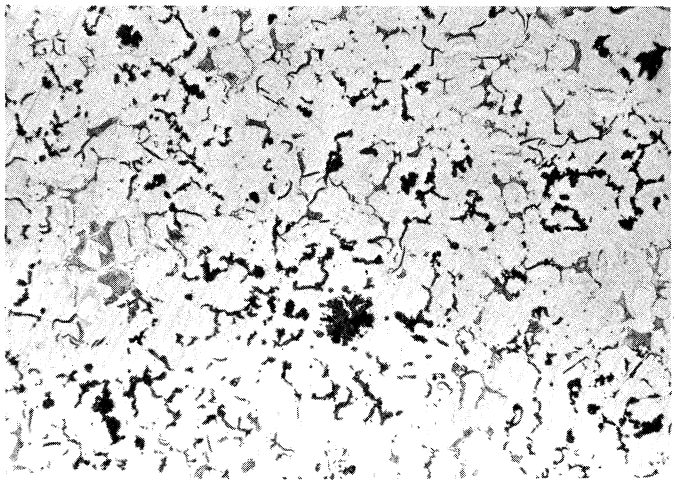

Fig. 27. 100X. 1/2" Y-block. MgAl; No late silicon; 2% Mo; 1% Al level. Heat 19.

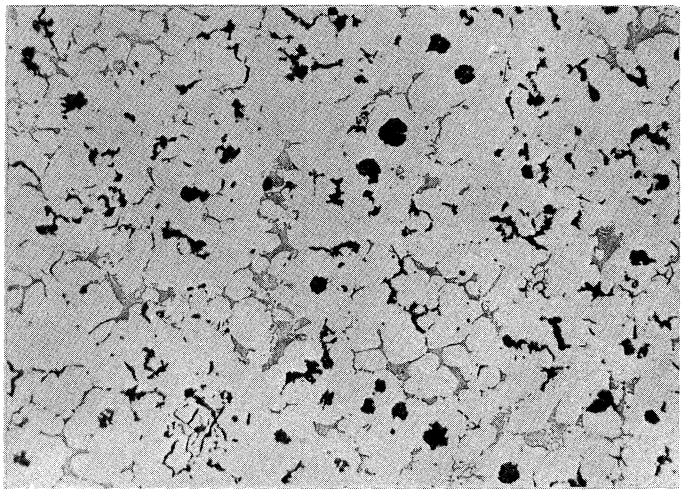

Fig. 28. 100X. 1/2" Y-block. MgAl; No late silicon; 0.02 Si added as mold inoculation; 2% Mo; 1% Al level. Heat 19.

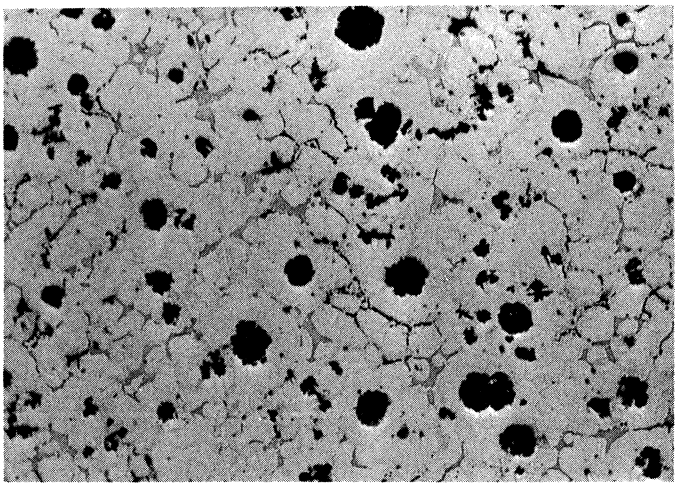

Fig. 29. 100X. 1/2" Y-block. CeMgFeSi; SMZ; 1.0 Si added as post inoculant; 2% Mo; 1% Al level. Heat 20.

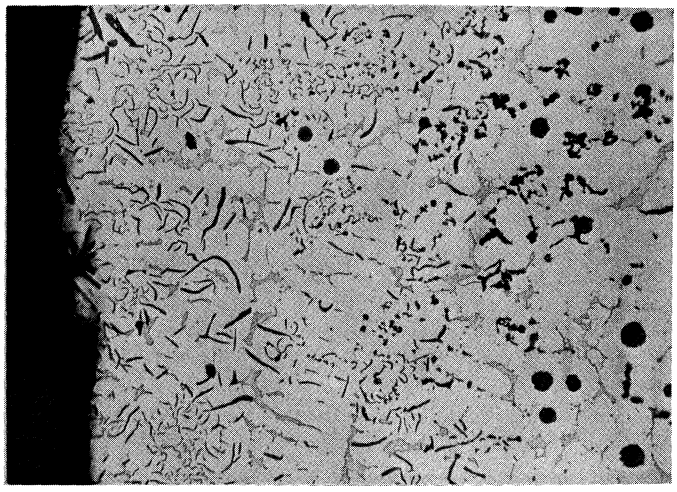

Fig. 30. 100X. 1/2" Y-block (edge). MgAl; SrFeSi (shows decay at sand interface); 2% Mo; 1% Al level. Heat 17.

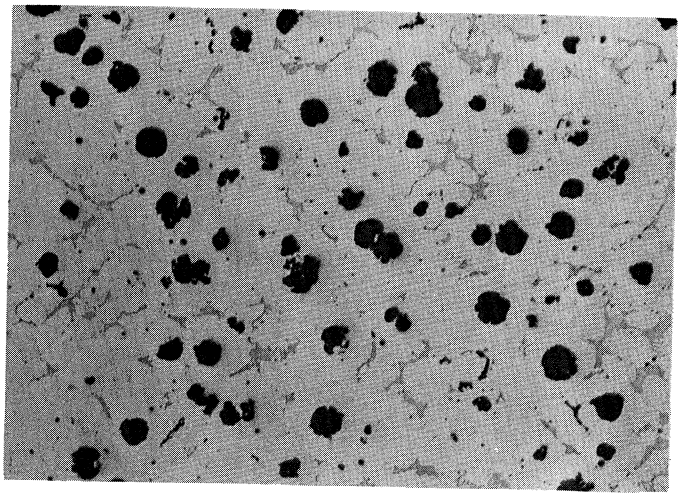

Fig. 31. 100X. 1/2" Y-block. MgFeSi; 75% FeSi; 2% Mo; 0% Al level. Heat 14.

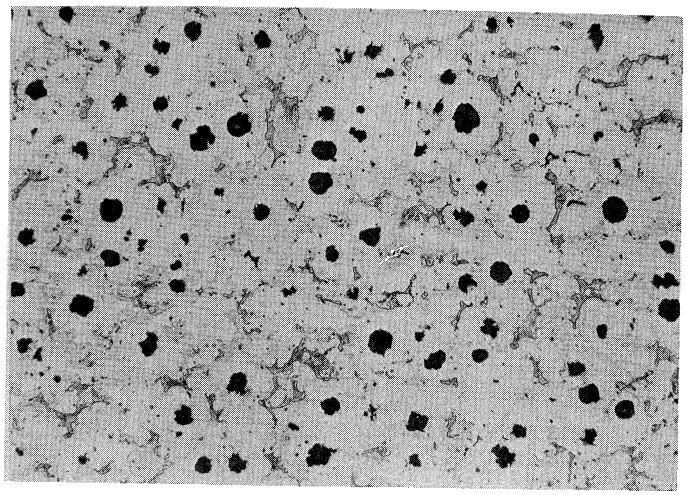

Fig. 32. 100X. 1/2" Y-block. As in Fig. 21 except 0.02 Si added as mold inoculant.

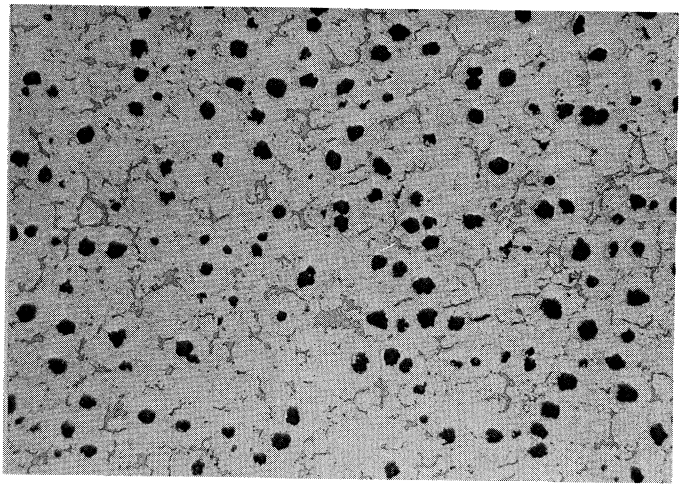

Fig. 33. 100X. 1/4" Y-block. Normalized 2 hours at 1850°F; MgFeSi; 75% FeSi; 2% Mo; 0% Al level. Heat 14.

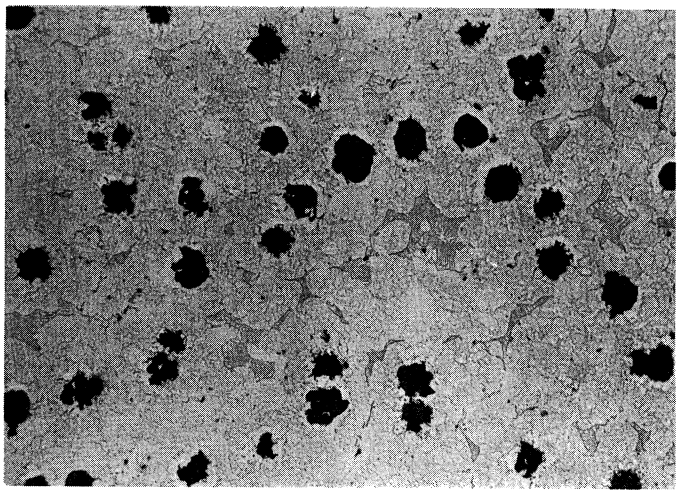

Fig. 34. 100X. 3" Y-block. Normalized 2 hours at 1750°F; MgFeSi; 75% FeSi; 2% Mo; 0% Al level. Heat 14.

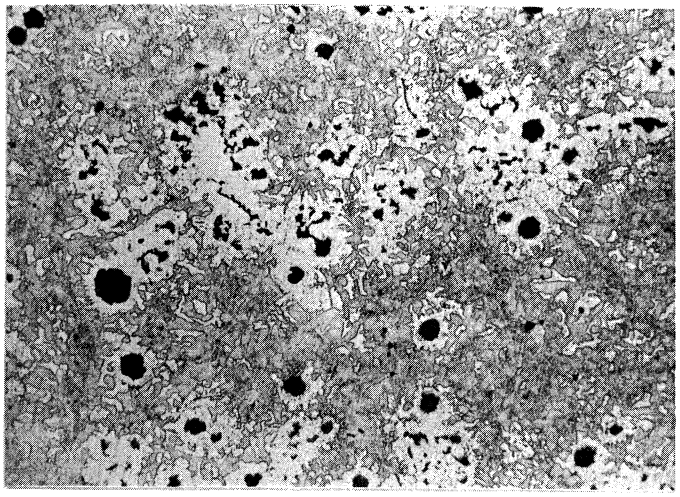

Fig. 35. 100X. 3" Y-block. Normalized 2 hours at 1850°F; MgFeSi; 75% FeSi; 2% Mo; 0% Al level. Heat 14.

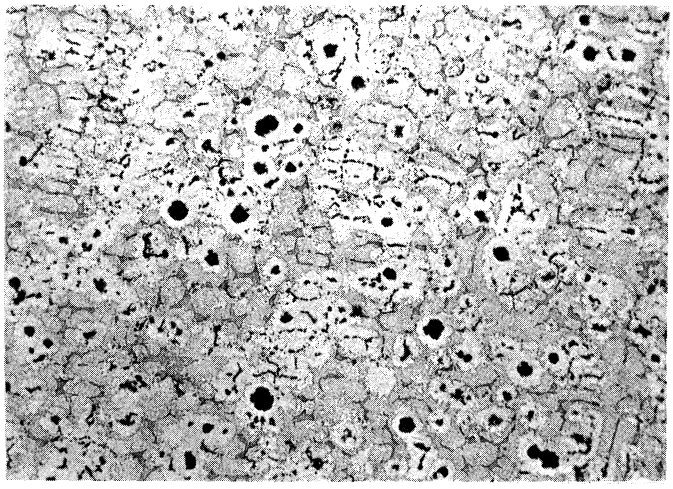

Fig. 36. 100X. 1/4" Y-block. Normalized 2 hours at 1850°F; MgFeSi; 75% FeSi; 2% Mo; 1% Al level. Heat 13.

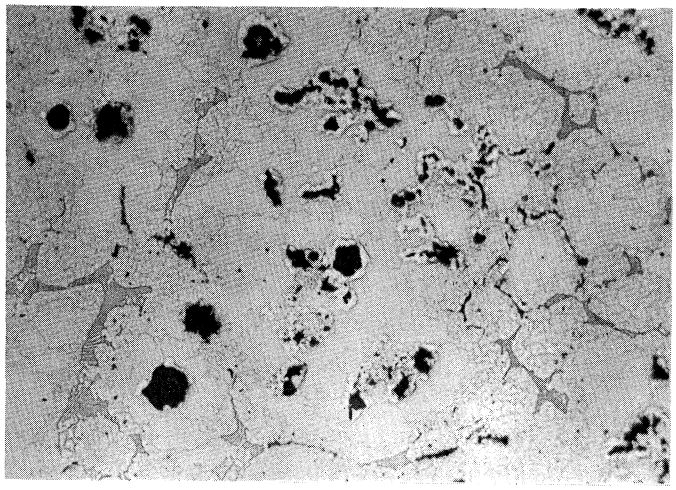

Fig. 37. 100X. 3" Y-block. Normalized 2 hours at 1750°F; MgFeSi; 75% FeSi; 2% Mo; 1% Al level. Heat 13.

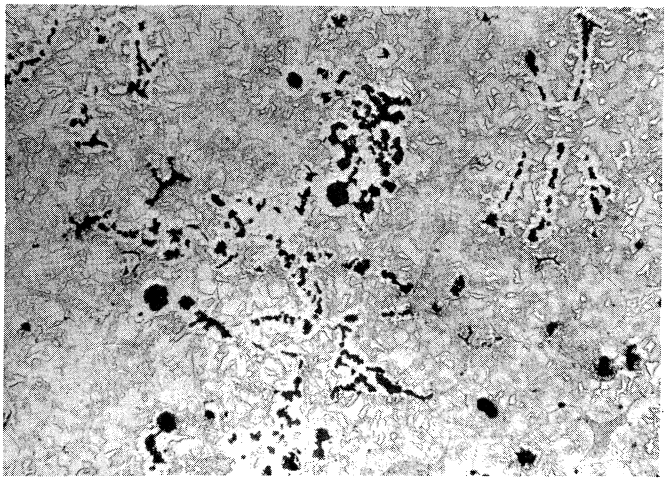

Fig. 38. 100X. 3" Y-block. Normalized 2 hours at 1850°F; MgFeSi; 75% FeSi; 2% Mo; 1% Al level. Heat 13.

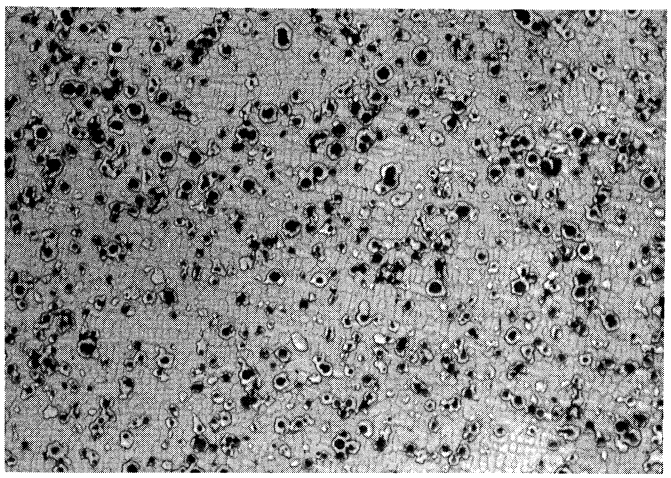

Fig. 39. 100X. Cast in 1" steel mold (Fig. 2). MgFeSi; 75% FeSi; 2% Mo; 1% Al level. Heat 13.

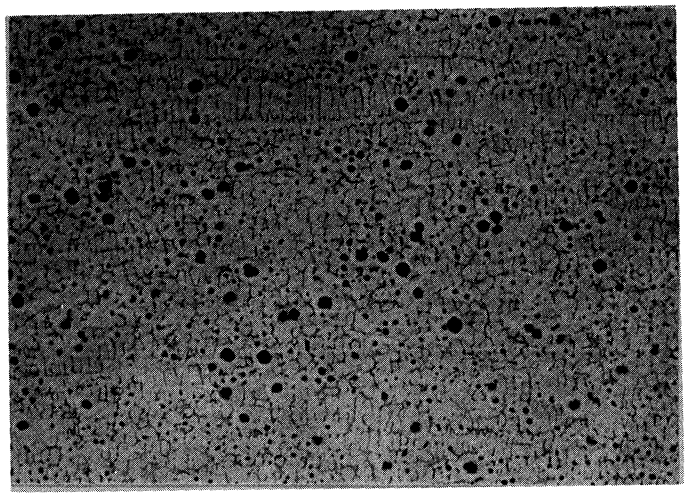

Fig. 40. 100X. Cast in 1" steel mold (Fig. 2). Normalized 6 hours at 1850°F; MgFeSi; 75% FeSi; 2% Mo; 1% Al level. Heat 13.